Interhead Distance Measurements in Myosin VI via SHRImP Support a Simplified Hand-Over-Hand Model

Hamza Balci,* Taekjip Ha,* H. Lee Sweeney,† and Paul R. Selvin*
*Physics and Biophysics Departments, University of Illinois, Urbana-Champaign, Illinois; and †University of Pennsylvania, Pennsylvania Muscle Institute, Philadelphia, Pennsylvania

ABSTRACT Myosin VI walks in a hand-over-hand fashion with an average step size of 30 nm, which is much larger than its 10 nm lever arm. Recent experiments suggest that the myosin VI structure has an unfolded and flexible region in the proximal tail which makes such a large step possible. In addition, cryoelectron microscopy images of actomyosin VI show the two heads bound to the actin monomers with a broad distribution of distances, including some as close as a few nanometers. This observation, when combined with the existence of a flexible region in the structure, which takes part in stepping, challenged the hand-over-hand model. In the hand-over-hand model, the lever arm is considered to be rigid and the interhead separation should not be very different from 30 nm. We considered an alternative model in which myosin VI heads sequentially take 60 nm steps whereas the interhead separation alternates between a large and small value (x and $60 - x$, where $x < 30$). To clarify these issues, we used a new technique, SHRImP, to measure the interhead distance of nearly rigor myosin VI molecules. Our data show a single peak at 29.3 ± 0.7 nm, in agreement with the straightforward hand-over-hand model.

INTRODUCTION

Myosin VI, similar to the other 17 members of the myosin superfamily (1), has three domains in its structure: a motor domain (N-terminal) that binds to actin and shows ATPase activity, a neck domain that binds light chains or calmodulin, and a tail domain (C-terminal) that binds to cargo. It was first discovered in *Drosophila* (2) and later was identified in many higher organisms ranging from *Caenorhabditis elegans* to humans (3–5). The gene for myosin VI is defective in the deaf mouse Snell's waltzer, suggesting that myosin VI is involved in the function of sensory hair cells (5,6). Myosin VI is unique in the myosin family in that it is the only member of the family that walks toward the pointed (minus) end of actin (7). It is also observed that myosin VI colocalizes with clathrin coated pits (8), which when combined with its directionality suggests that it is involved in endocytosis (9).

Recently myosin VI has attracted attention due to two of its unusual properties—processivity and step size. Biochemical characterization and electron microscopy studies on myosin VI have shown that expressed full-length myosin VI is a monomer and is a nonprocessive motor (10). However, it has also been shown that dimerized myosin VI can take many steps before detaching from actin (11–14), and hence acts as a processive motor. It is not clear at this point how myosin VI functions within the cell: as a monomer, a dimer, or both. However, extensive optical trap experiments on myosin VI imply a possible explanation by attributing multifuntionality, which might require both monomers and dimers of this motor (15). The molecules that we use in this study are dimerized constructs of myosin VI. The second unusual property of myosin VI, which is the topic of this article, was realized when motility experiments on dimerized constructs of myosin VI measured a step size that is not compatible with the assumed structure of this motor using the well-established lever arm mechanism (11–14).

The hand-over-hand model of walking using a lever arm mechanism has been well established for processive motors in the myosin and kinesin families (16–24). The step of these molecular motors consists of two parts: a power stroke and a diffusive search that follows the power stroke (22). The size of the power stroke is comparable to the size of the light chain domain which acts as the lever arm. For example for myosin V, the step is formed from a ~23 nm (size of the light chain domain) power stroke and a ~12 nm diffusive search (22). However, in the case of myosin VI the situation is quite different since the light chain domain (~10 nm) is much shorter than the measured step size (~30 nm; 13,14). Two possible scenarios were considered: there is a rigid extension to the lever arm which would enable a longer power stroke, or there is a flexible compliant region which enables the motor to go through a longer diffusive search. Several experimental observations (13,25) favor the proximal tail to act as a flexible compliant region rather than a rigid extension to the lever arm. The emerging picture is that, after the power stroke of the motor (~12 nm), the head domain goes through a biased diffusive search on the actin monomer (~20 nm) until it finds the next binding site.

The complications in myosin VI motility were further increased with cryoelectron microscopy images of myosin VI.

Submitted February 3, 2005, and accepted for publication April 26, 2005.

Address reprint requests to Paul R. Selvin, Loomis Laboratory of Physics, 1110 W. Green St., University of Illinois, Urbana, IL 61801. Tel.: 217-244-3371; Fax: 217-244-7187; E-mail: selvin@uiuc.edu.

0006-3495/05/07/413/05 $2.00

doi: 10.1529/biophysj.105.060608

These images showed that for some of the motors, the two heads of the dimer were bound to adjacent actin monomers with a separation much less than 30 nm (12). These images, when considered with the additional degree of freedom provided by the flexible region in the proximal tail domain, challenged the hand-over-hand model of walking. Fig. 1 *b* shows an alternative model where the heads alternately take 60 nm steps and the distance between the heads is either x nm or $60 - x$ nm, depending on which head took the last step, where x could have any value between ~5 nm (since the two heads cannot be on the same actin monomer) and 30 nm (Fig. 1 *b*). This model will be referred to as the asymmetric hand-over-hand model in the rest of the article. To clarify this issue we measured the separation between the myosin VI heads, rather than the step size. In the hand-over-hand model, we would expect the interhead separation to show a single peak at 30 nm, whereas the asymmetric hand-over-hand model should show two peaks: one at x nm and another at $60 - x$ nm. We used our recently introduced single-molecule high resolution imaging with photobleaching (SHRImP) to determine the distance between enhanced green fluorescent protein (eGFP) molecules on the heads of myosin VI with nanometer precision (26,27).

MATERIALS AND METHODS

Imaging

Olympus (Melville, NY) IX-71 microscope, Olympus Apo 100×, 1.65 numerical aperture oil objective, and high refractive index coverslips (also from Olympus) were used in the objective type total internal reflection setup. The eGFP molecules were excited using a Melles Griot (Carlsbad, CA) ion laser at 488 nm wavelength. Images were captured by using a slow-scan back-thinned Andor Technology (South Windsor, CT) charge-coupled device camera, allowing continuous imaging with no interframe dead time. The image capture frequency was 2 Hz (13).

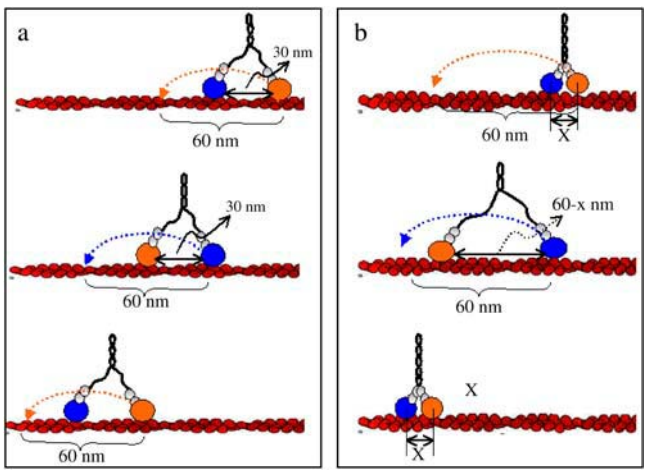

FIGURE 1 (*a*) Hand-over-hand mechanism of walking. (*b*) An alternative model of motility in which the separation between the myosin heads alternates between x and $60 - x$ nm, whereas each head takes 60 nm steps sequentially. Cryoelectron microscopy images suggest that x could be much less than 30 nm.

Sample preparation

The samples were prepared as described in Yildiz et al. (13). The sapphire coverslips and glass slides were sonicated in acetone for 20 min, rinsed with doubly deionized water, sonicated in 1 M KOH for another 20 min, and finally rinsed again with doubly deionized water. The sample chamber was prepared by flowing 10 mM bovine serum albumin-biotin, waiting for 10 min, washing with M5BufBH (20 mM HEPES pH 7.6, 2 mM MgCl2, 25 mM KCl, 1 mM EGTA), followed by 0.5 mg/ml streptavidin, waiting for 5 min, followed by 0.2 μM 1:10 biotinylated/unbiotinylated phalloidin-stabilized F-actin, followed by M5+ (M5BufBH plus 10 mM DTT and 100 mg/ml calmodulin) wash, followed by myosin VI sample solution. Myosin VI sample solution consists of 50 pM eGFP-myosin VI, 100 mM DTT, 100 mg/ml calmodulin, and 1–2 μM ATP, in M5BufBH.

Data analysis

We have used SHRImP (26) to measure the distance between the myosin VI heads in the presence of very low concentrations of ATP. SHRImP takes advantage of quantal photobleaching of fluorescent molecules to resolve two fluorophores which lie on the same plane and which have overlapping point spread functions (PSFs). In this case, there would be a two-step photobleaching event, and each of the steps corresponds to the photobleaching of one of the dyes. The images both before and after photobleaching of one of the dyes are fit to two dimensional Gaussian functions. The image after one of the dyes photobleaches is used to determine the PSF of one of the dyes, and the difference between this image and the one before the first photobleaching is used to determine the PSF of the other dye. Hence, both dyes can be simultaneously localized by using this simple idea.

RESULTS AND DISCUSSION

We used SHRImP to measure the distance between the myosin VI heads. The fluorophores are two eGFPs located at the N-terminus, or head region, of the myosin VI dimer. The data are taken in the presence of very low concentrations of ATP to make sure the myosin heads are bound to the actins in a configuration relevant for stepping (1 μM, which is ~3% of that used for motility experiments). However, the concentration of ATP is low enough that almost all of the dyes are stationary. Among the thousands of molecules we imaged in the course of this study, we noticed only a few which moved 1–2 steps. These were not included in the analysis. This is a necessary condition to be able to measure the separation between the two heads accurately and avoid any confusion that could result from the moving of one or both heads during the measurement. Since the myosin molecules do not move, it is important to make sure that they land on actins rather than nonspecifically bind to the surface. To test if any nonspecific binding occurs, the actins were decorated with a high concentration of myosin VI molecules. We include an image of the actin filaments decorated with myosin VI molecules as Supplementary Online Material. This image clearly shows that the myosin molecules bind only to the actins and not to the surface. In addition, the actin concentration is low enough and the length of the actin where multiple actins cross over is far shorter than the full-length of the actin filaments to assure us that a myosin VI molecule would bind to only one actin filament.

Fig. 2 *a* shows an example of two-step photobleaching. The intensity on the *y* axis corresponds to the maximum of the PSF although the same two-step photobleaching can be observed in the total integrated area under the PSF as well. Fig. 2 *b* shows the corresponding PSFs before and after photobleaching. The difference between the first two graphs is shown in the third graph, which is the PSF of the eGFP that photobleached first. The details of the data analysis using SHRImP are given in Gordon et al. (26).

The frequency of the two-step photobleaching events was sensitively dependent on the experimental conditions used in preparing the sample. However, 1–2% was the typical frequency that showed clear two-step photobleaching. In the best cases, this frequency was as high as 5%. Most of the dyes showed a single step photobleaching. It is not clear at this point why higher frequency of two-step photobleaching could not be observed, since in gel filtration experiments our samples showed a single band of doubly labeled myosin VI (data not shown). However, there are several reasons which would reduce the frequency of observing clear two-step photobleaching events. The relatively long integration time we use in acquiring the images is one of these reasons. The images were taken every 0.5 s; therefore if the dyes photobleached one after another within 1–2 s, we would not be able to clearly distinguish this event from a single step photobleaching event. In addition, it is possible that one of the dyes photobleached within the first 1–2 s after the laser is turned on. This case would not be counted as a two-step photobleaching event since the time is too short to get reliable statistics. In a few rare cases we observed broad, rather than single step, photobleaching events, which indicates that the myosins formed aggregates. We submit an image as Supplementary Online Material showing the concentration of myosin VI molecules we used in the experiments. As is clear in this image, the concentration of myosin VI molecules is low enough to image single molecules.

Fig. 3 shows a histogram of the separation between the myosin VI heads determined from the two-step photobleaching events and various fits made to this histogram. There are 96 points in the histogram. The average interhead separation of the 96 molecules is 31.0 nm, and the SD is 15.4 nm. Each point reflects an average distance determined from the best Gaussian fits to several pre- and postphotobleach events. Typically, four frames were used to compute the average distance. However, in some cases only two frames yielded good enough fits that could be used, and in some cases as many as nine frames were used to find the average distance. The center of a Gaussian for each frame was typically determined within an error of 5–6 nm. The best resolution (in localizing the center of the Gaussian) obtained was 3 nm, and the minimum acceptable resolution (to be included in the histogram) was 10 nm.

The curves in Fig. 3 are three different fits to the data. Different fits were used to model the alternative walking styles presented in Fig. 1. In the case of the symmetric hand-over-hand model, we would expect the interhead separation to peak at 30 nm, and hence a single Gaussian should be able to represent the histogram. A Gaussian fit of the form $y = y_0 + a \exp[-0.5 \times ([x - x(0)]/b)^2]$ to the histogram results in $x(0) = 29.2 \pm 0.8$ nm, which is in very good agreement

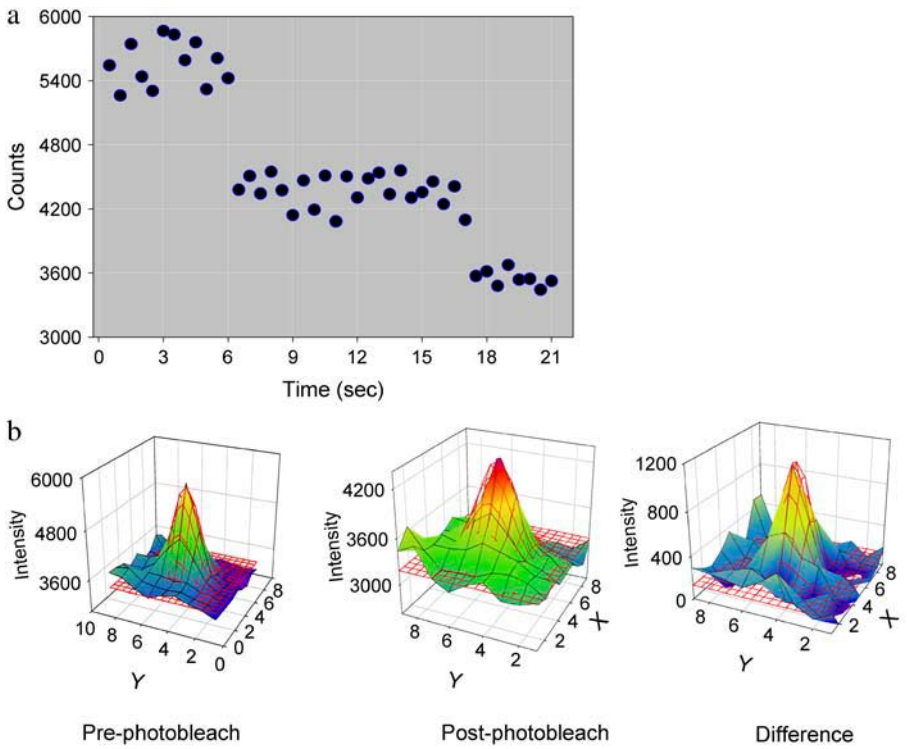

FIGURE 2 (*a*) Peak intensity versus time for a myosin VI dimer labeled with two eGFPs. (*b*) Pre- and postphotobleach of one of the eGFPs. The last graph shows the difference between the first two, which is the emission from the eGFP that photobleached first.

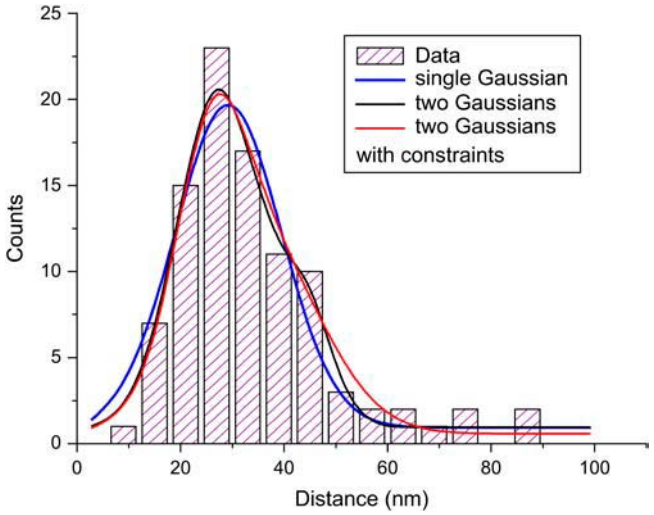

FIGURE 3 Histogram of measured separations between the myosin VI heads and three Gaussian fits to the data. The blue curve is a single Gaussian fit representing the hand-over-hand model, the black curve is an unconstraint fit of two Gaussians, and the red curve is a fit of two Gaussians with constraints.

with the symmetric hand-over-hand model. The other parameters generated by the fit are $y_0 = 0.9 \pm 0.6$ nm, $a = 19.9 \pm 1.4$, and $b = 9.7 \pm 0.9$ nm. The full width at half maximum of the Gaussian is 23.8 nm. However, the broadness of the peak we observe in the histogram and in the corresponding Gaussian fit suggests that two closely spaced Gaussians may be able to describe the data as well. To study this possibility further, we fit the data with a function of the form $y = y_0 + a \exp[-0.5 \times ([x - x_1(0)]/b)^2] + c \exp[-0.5 \times ([x - x_2(0)]/d)^2]$. This fit is shown as the black curve in Fig. 2, and the corresponding parameters are $y_0 = 0.9 \pm 0.3$ nm, $a = 21.7 \pm 0.9$, $x_1(0) = 27.3 \pm 0.5$ nm, $b = 7.2 \pm 0.5$ nm, $c = 8.2 \pm 1.3$, $x_2(0) = 43.9 \pm 1.0$ nm, and $d = 4.2 \pm 0.7$ nm. This function corresponds to a model in which the separation between the heads alternate between 27.3 nm and 43.9 nm. This would suggest that even if the asymmetry between the interhead separations is as large as $43.9 - 27.3 = 16.6$ nm, we would not be able to distinguish it from the symmetric case presented earlier. Even though the data seem to be very well described by such a fitting function (Reduced $\chi^2 = 1.0$), the amplitudes of the Gaussians, which is a measure of the frequency of observing the corresponding interhead separation, do not represent the experimental conditions we used. The amplitude of the Gaussian for 27.3 nm interhead separation is 21.7 and the amplitude for 43.9 nm separation is 8.2, which means that 73% of the time we observe the myosins when the interhead separation is 27.3 nm. However, there is no reason for such a strong bias in the statistics to happen toward one of the interhead separation, and on average we should observe the two interhead separations with equal frequency. Another problem with this fit is that 27.3 nm and 43.9 nm result in a step size of 35.6 nm, which is significantly larger than the expected 30 nm step. A more realistic fit which consists of two Gaussians would be one in which the amplitudes of the Gaussians are equal to each other ($a = c$ in the previous function), and the sum of the two separations equals 60 nm (the *red curve* in Fig. 3). Such a fit, $y = y_0 + a \exp[-0.5 \times ([x - x_1(0)]/b)^2] + a \exp[-0.5 \times ([x - (60 - x_1(0))]/d)^2]$, is shown as the red line in Fig. 2. The parameters of the function are determined to be $y_0 = 0.6 \pm 0.5$ nm, $a = 12.0 \pm 0.8$, $x_1(0) = 34.3 \pm 0.9$ nm, $b = 11.6 \pm 1.6$ nm, and $d = 5.5 \pm 0.7$ nm, and the reduced $\chi^2 = 1.5$. According to this fit, the peaks of the Gaussians are at 34.3 nm and 25.7 nm, which result in an asymmetry of 8.6 nm. Hence, the resolution of our data in separating two peaks from one would be somewhere between 8.6 nm and 16.6 nm. A nonrigorous and conservative estimate for resolution would be 14 nm.

CONCLUSION

Our results are the first application of SHRImP on motor proteins, and they represent the unique capabilities of this technique in measuring distances between 10 nm and 100 nm. We show that in the presence of very low concentrations of ATP the separation between the heads of myosin VI is 29.3 ± 0.7 nm, in agreement with the straightforward hand-over-hand model. Although the distribution in the measured head-to-head separation does not allow us to rule out a small asymmetry, we can set an upper limit of 14 nm for this asymmetry in the interhead separation (i.e., the interhead separation cannot be more asymmetric than $x_1(0) = 23$ nm and $x_1(0) = 37$ nm). Since such large separations between the heads are structurally not possible by considering only the light chain domains (the maximum possible separation a 10 nm long lever arm can provide is $10 + 10 = 20$ nm), the flexible region which enables the 60 nm step should also be at least partially open in between steps as well.

SUPPLEMENTARY MATERIAL

An online supplement to this article can be found by visiting BJ Online at http://www.biophysj.org.

We thank Matthew Gordon for sharing his SHRImP software with us, and Hyokeun Park and Ahmet Yildiz for their instructions regarding the sample preparation. We thank Anna Li and Damien Garbett for protein preparation.

This work was supported by National Institutes of Health grants AR44420, AR48931, and GM68625, and National Science Foundation grants DBI-02-15869 and 0134916.

REFERENCES

1. Berg, J. S., B. C. Powell, and R. E. Cheney. 2001. A millennial myosin census. *Mol. Biol. Cell.* 12:780–794.
2. Kellerman, K. A., and K. G. Miller. 1992. An unconventional myosin heavy chain gene from *Drosophila* melanogaster. *J. Cell Biol.* 119: 823–834.

3. Hasson, T., and M. S. Mooseker. 1994. Porcine myosin VI: characterization of a new mammalian unconventional myosin. *J. Cell Biol.* 127:425–440.

4. Avraham, K. B., T. Hasson, T. Sobe, B. Balsara, J. R. Testa, A. B. Skvorak, C. C. Morton, N. G. Copeland, and N. A. Jenkins. 1997. Characterization of unconventional MYO6, the human homologue of the gene responsible for deafness in Snell's waltzer mice. *Hum. Mol. Genet.* 6:1225–1231.

5. Avraham, K. B., T. Hasson, K. P. Steel, D. M. Kingsley, L. B. Russell, M. S. Mooseker, N. G. Copeland, and N. A. Jenkins. 1995. The mouse Snell's waltzer deafness gene encodes an unconventional myosin required for structural integrity of inner ear hair cells. *Nat. Genet.* 11: 369–375.

6. Hasson, T., P. G. Gillespie, J. A. Garcia, R. B. MacDonald, Y. Zhao, A. G. Yee, M. S. Mooseker, and D. P. Corey. 1997. Unconventional myosins in inner-ear sensory epithelia. *J. Cell Biol.* 137:1287–1307.

7. Wells, A. L., A. W. Lin, L. Q. Chen, D. Safer, S. M. Cain, T. Hasson, B. O. Carragher, R. A. Milligan, and H. L. Sweeney. 1999. Myosin VI is an actin-based motor that moves backwards. *Nature.* 401:505–508.

8. Buss, F., S. D. Arden, M. Lindsay, J. P. Luzio, and J. Kendrick-Jones. 2001. Myosin VI isoform localized to clathrin-coated vesicles with a role in clathrin-mediated endocytosis. *EMBO J.* 20:3676–3684.

9. Aschenbrenner, L., T. Lee, and T. Hasson. 2003. Myo6 facilitates the translocation of endocytic vesicles from cell peripheries. *Mol. Biol. Cell.* 14:2728–2743.

10. Lister, I., S. Schmitz, M. Walker, J. Trinick, F. Buss, C. Veigel, and J. Kendrick-Jones. 2004. A monomeric myosin VI with a large working stroke. *EMBO J.* 23:1729–1738.

11. Rock, R. S., S. E. Rice, A. L. Wells, T. J. Purcell, J. A. Spudich, and H. L. Sweeney. 2001. Myosin VI is a processive motor with a large step size. *Proc. Natl. Acad. Sci. USA.* 98:13655–13659.

12. Nishikawa, S., K. Homma, Y. Komori, M. Iwaki, T. Wazawa, A. Hikikoshi Iwane, J. Saito, R. Ikebe, E. Katayama, T. Yanagida, and M. Ikebe. 2002. Class VI myosin moves processively along actin filaments backward with large steps. *Biochem. Biophys. Res. Commun.* 290:311–317.

13. Yildiz, A., H. Park, D. Safer, Z. Yang, L. Q. Chen, P. R. Selvin, and H. L. Sweeney. 2004. Myosin VI steps via a hand-over-hand mechanism with its lever arm undergoing fluctuations when attached to actin. *J. Biol. Chem.* 279:37223–37226.

14. Okten, Z., L. S. Churchman, R. S. Rock, and J. A. Spudich. 2004. Myosin VI walks hand-over-hand along actin. *Nat. Struct. Mol. Biol.* 11:884–887.

15. Altman, D., H. L. Sweeney, and J. A. Spudich. 2004. The mechanism of myosin VI translocation and its load-induced anchoring. *Cell.* 116: 737–749.

16. Mehta, A. D., R. S. Rock, M. Rief, J. A. Spudich, M. S. Mooseker, and R. E. Cheney. 1999. Myosin V is a processive actin-based motor. *Nature.* 400:590–593.

17. Yildiz, A., M. Tomishige, R. D. Vale, and P. R. Selvin. 2004. Kinesin walks hand-over-hand. *Science.* 303:676–678.

18. Yildiz, A., J. N. Forkey, S. A. McKinney, T. Ha, Y. E. Goldman, and P. R. Selvin. 2003. Myosin V walks hand-over-hand: single fluorophore imaging with 1.5-nm localization. *Science.* 300:2061–2065.

19. Sakamoto, T., I. Amitani, E. Yokota, and T. Ando. 2000. Direct observation of processive movement by individual myosin V molecules. *Biochem. Biophys. Res. Commun.* 272:586–590.

20. Purcell, T. J., C. Morris, J. A. Spudich, and H. L. Sweeney. 2002. Role of the lever arm in the processive stepping of myosin V. *Proc. Natl. Acad. Sci. USA.* 99:14159–14164.

21. Mehta, A. 2001. Myosin learns to walk. *J. Cell Sci.* 114:1981–1998.

22. Veigel, C., F. Wang, M. L. Bartoo, J. R. Sellers, and J. E. Molloy. 2002. The gated gait of the processive molecular motor, myosin V. *Nat. Cell Biol.* 4:59–65.

23. Forkey, J. N., M. E. Quinlan, M. A. Shaw, J. E. Corrie, and Y. E. Goldman. 2003. Three-dimensional structural dynamics of myosin V by single-molecule fluorescence polarization. *Nature.* 422:399–404.

24. Warshaw, D. M., G. Kennedy, S. Work, E. Krementsova, S. Beck, and K. Trybus. 2005. Differential labeling of myosin V heads with quantum dots allows direct visualization of hand-over-hand processivity. *Biophys. J.* 88:L30–L32.

25. Rock, R. S., B. Ramamurthy, A. R. Dunn, S. Beccafico, B. R. Rami, C. Morris, B. J. Spink, C. Franzini-Armstrong, J. A. Spudich, and H. L. Sweeney. 2005. A flexible domain is essential for the large step size and processivity of myosin VI. *Mol. Cell.* 17:603–609.

26. Gordon, M. P., T. Ha, and P. R. Selvin. 2004. Single-molecule high-resolution imaging with photobleaching. *Proc. Natl. Acad. Sci. USA.* 101:6462–6465.

27. Qu, X., D. Wu, L. Mets, and N. F. Scherer. 2004. Nanometer-localized multiple single-molecule fluorescence microscopy. *Proc. Natl. Acad. Sci. USA.* 101:11298–11303.